

PROCEEDINGS OF SPIE

[SPIDigitalLibrary.org/conference-proceedings-of-spie](https://spiedigitallibrary.org/conference-proceedings-of-spie)

Optofluidic microscope: a complete on-chip imaging device

Xiquan Cui, Xin Heng, Changhui Yang

Xiquan Cui, Xin Heng, Changhui Yang, "Optofluidic microscope: a complete on-chip imaging device," Proc. SPIE 6859, Imaging, Manipulation, and Analysis of Biomolecules, Cells, and Tissues VI, 68590Y (29 February 2008); doi: 10.1117/12.764957

SPIE.

Event: SPIE BiOS, 2008, San Jose, California, United States

Optofluidic Microscope - A Complete On-Chip Imaging Device

Xiquan Cui^{1*}, Xin Heng¹, Changhui Yang¹

¹Electrical Engineering, California Institute of Technology, Pasadena, CA 91125;

ABSTRACT

This paper reports a complete on-chip high resolution lensless imaging device based on the optofluidic microscopy method, which can form a vital optical microscopy component in a wide range of lab-on-a-chip systems. This imaging device does not use any lens elements and yet is capable of resolution comparable to that of a conventional microscope with a 20× objective. We demonstrate the use of the device for *Caenorhabditis elegans* and microsphere imaging at a resolution of $\sim 1 \mu\text{m}$ with an imaging time of ~ 2 sec. The fabrication of this on-chip imaging device is fully compatible with existing semiconductor and microfluidic technologies, so the device can be massively fabricated and integrated into microsystems to form compact and low-cost total analysis systems for biological and colloidal studies.

Keywords: Microscope, optofluidics, cytometry, microorganism, colloid, biophotonics, microfluidics.

1. Introduction

The major advantages of the microfluidic lab-on-a-chip systems are their inherent compactness, low cost, high resolution and sensitivity, which makes them suitable for both portable and point-of-need devices to replace centralized laboratories. But as pointed out in references¹⁻³, while excellent solutions to important miniaturization challenges in the lab-on-a-chip systems have been recently brought forward and demonstrated, one particular on-chip instrumentation need has not been satisfactorily addressed – high resolution ($\sim 1 \mu\text{m}$ or better) on-chip optical imaging. High resolution imaging requirement in existing lab-on-a-chip systems still relies on using off-chip and bulky conventional optical microscope, which obviates the size and cost advantages of the lab-on-a-chip systems. The size and cost disadvantages of current optical microscope systems intrinsically root from the conventional microscopy method, which requires sophisticated lens systems to correct aberrations and large space to relay images. The optofluidic microscopy (OFM) method, developed in our group³, abandons the conventional microscopy concept, and adapts the simple direct projection imaging scheme to overcome the drawbacks induced by the conventional optical microscopy. The operating principle of OFM is very simple (Fig. 1b). We use a linear CCD or CMOS imaging sensor array as the photon sensing substrate. We coat it with a thin metal film to block the light, and redefine a slanted line of equal spaced small apertures on the metal film. Each aperture corresponds to an imaging sensor pixel, and each pixel can only detect the light transmitted through the corresponding aperture. On top of the linear CCD, we stack an optically transparent microfluidic channel. So when we flow cells or microorganisms through the microfluidic channel, each pixel will record a different line profile of the transmission image of the biological sample through the corresponding aperture. By stacking the line traces together appropriately, we can form an image of the object. Because of the simple aperture based direct projection imaging scheme, no lens and large space are needed to form high resolution images, and compact and low cost on-chip imaging device can be implemented.

The direct projection imaging scheme on a CMOS photon sensor array has been demonstrated by Lange, D. et al⁴. In their method, the specimen was placed directly on top of a CMOS image sensor, and the projection image of the specimen was then recorded by the sensor pixels underneath. However, since

* Email: xiquan@caltech.edu

generally the pixel size of a commercial CCD or CMOS sensor is about $5\ \mu\text{m}$ or larger, the resolution of such devices is insufficient for a wide range of biological imaging applications. In addition, because the pixels in CCD and CMOS sensors must be physically separated, the sparse sampling could introduce severe aliasing in digitized images⁵. In the OFM imaging scheme, the resolution is only limited by the size of the apertures defined on the metal film above the imaging sensor pixels. With current fabrication techniques, submicron apertures can be readily fabricated. So high resolution on-chip imaging is achievable with OFM method. The arrangement of the small apertures with respect to the microfluidic flow is another key novelty of the OFM imaging scheme. Along the Y axis, perpendicular to the microfluidic flow direction, the sampling of OFM is adjustable by changing the tilt angle θ between the line of apertures and the microfluidic flow direction. For a specimen smaller than the imaging sensor pixel, in a non-OFM sampling scheme, spatially there is only one sampling point along Y axis, which yields an image with poor quality (Fig. 1a); but in the OFM sampling scheme, dense sampling in Y direction can be achieved by choosing a proper tilt angle θ (Fig. 1b). The sampling in the microfluidic flow direction X can be improved by increasing the frame rate of the imaging sensor array underneath. The aliasing caused by image digitization can be well controlled in the OFM imaging scheme.

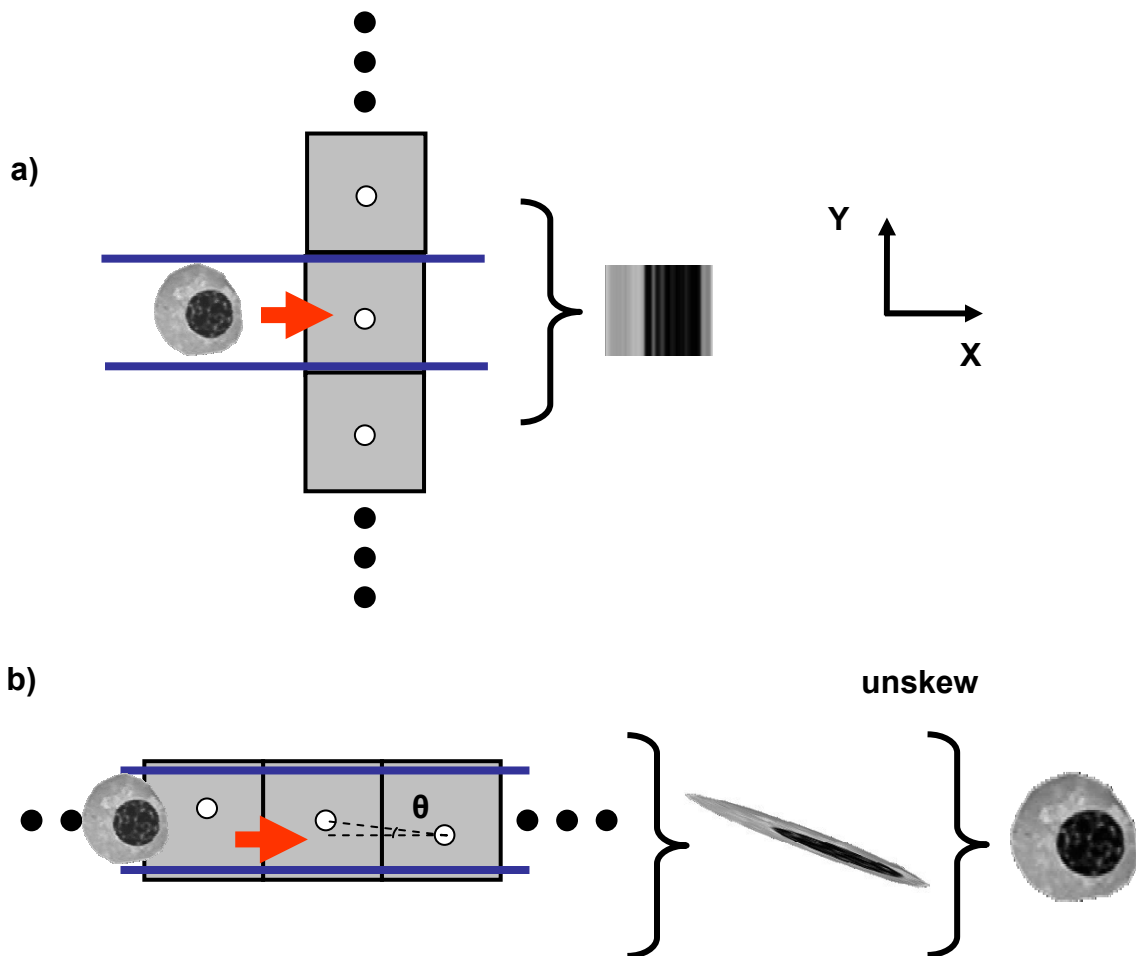


Figure 1: **a.** A non-OFM imaging scheme yields an image with poor quality because of the sparse sampling in the Y direction. **b.** OFM imaging scheme can achieve dense sampling in the Y direction by choosing a proper tilt angle θ .

In this report, we present, to our knowledge, the first complete on-chip lensless high resolution optical microscopy device ever reported. Our whole on-chip OFM prototype is about the size of a dime, and yet is capable of resolution comparable to that of a conventional microscope with a 20× objective lens. In the next section, we will describe the architecture of the OFM prototype and its operating principle. Then, we will demonstrate the application of OFM on-chip imaging capability in both biological and colloidal researches by imaging both *Caenorhabditis elegans* (*C. elegans*) and polystyrene microspheres. Finally, we will conclude the manuscript by describing some other appropriate applications of such on-chip microscope device and more functions we can add into the OFM imaging family.

2. Method

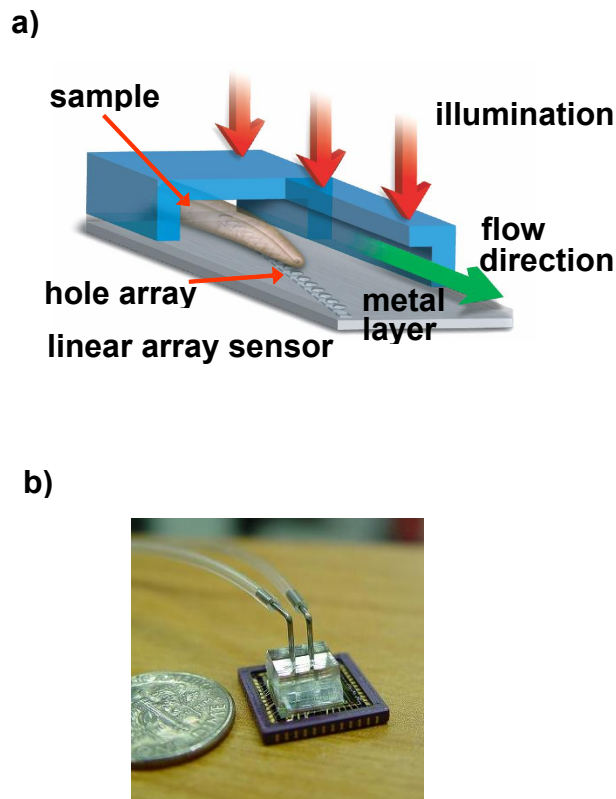


Figure 2: **a.** The schematics showing the working principle of the OFM device. **b.** A typical on-chip OFM prototype device, which is about the size of a dime.

Fig. 2a is the schematics showing the working principle of OFM device. At the bottom is an imaging sensor as the substrate. A metal layer is coated on top to screen out the light. A slanted line of small apertures are punched to limit each sensor pixel to sample the light only transmitted through the corresponding aperture. A transparent polydimethylsiloxane (PDMS) microfluidic channel is stacked on top of the sensing substrate to guide the specimen solution to pass the OFM aperture array at the designed tilt angle to ensure proper sampling. The light source illuminates the whole OFM device uniformly from above. Fig. 2b shows a typical on-chip OFM prototype device. The whole OFM device is about the size of a dime.

The on-chip OFM imaging device is a complete micro-opto-electromechanical systems (MOEMS) system which contains optical projection, fluidic transportation, and electronic detection and data acquisition functionalities. Compatibility is an important issue for successfully integrating modules with different properties. A series of low temperature and mild processes have been used to realize our complete on-chip OFM devices.

We used a commercially available 2D CMOS imaging sensor (Micron MT9V403C12STM) instead of a linear sensor, because few linear sensors with big substrate are available and with 2D sensor chip multiple OFM arrays can be implemented on a single chip. But during the OFM imaging experiment, we only assign a row of sensor pixels to an OFM aperture array. So each OFM array still works in the same way as we described before.

The sensor pixel size is $9.9\ \mu\text{m} \times 9.9\ \mu\text{m}$ (Fig. 3a). The electrodes surrounding a sensor pixel are about $1.2\ \mu\text{m}$ higher than the center of the pixel. In order to maintain uniform microfluidic flow for perfect OFM imaging, we spun a $2\ \mu\text{m}$ thick layer of SU8 photoresist to planarize the surface of the CMOS sensor die (Fig. 3b). After 3 minutes 95°C pre-bake, 1 minute UV curing, 3 minutes 95°C post-exposure bake, and 150°C hard bake, the corrugation of the surface topography of the sensor die is less than 80nm . Later success OFM imaging shows that the sensing substrate is flat enough to support uniform microfluidic flow for OFM imaging. Then we coated the planarized sensing substrate with a 300nm thick layer of Al to mask the CMOS pixels from light (Fig. 3c) with a thermal evaporator (Caltech Watson cleanroom). Finally, we used focused ion beam (FIB) machine (Nova 200, FEI Company) to punch the OFM apertures with $1\ \mu\text{m}$ diameter on the Al thin film (Fig. 3d).

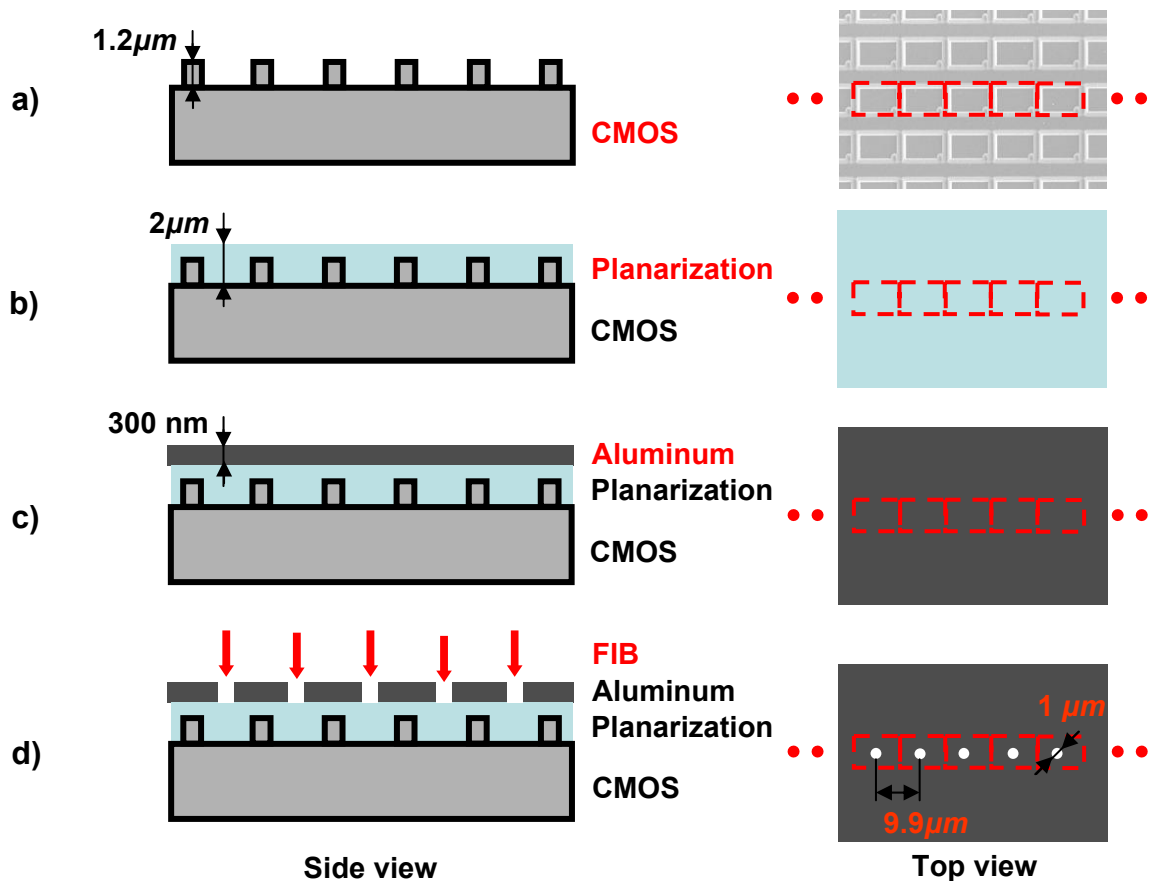


Figure 3: **a.** The raw CMOS image sensor with $9.9\ \mu\text{m} \times 9.9\ \mu\text{m}$ pixel size and $1.2\ \mu\text{m}$ high corrugation on the surface of the CMOS sensor die. **b.** A $2\ \mu\text{m}$ thick layer of SU8 photoresist is spun on to planarize the surface of the CMOS sensor die, the corrugation of the surface topography of the sensor die is less than 80nm after the planarization process. **c.** 300nm thick layer of Al is coated on the planarized sensing substrate to mask the CMOS pixels from light by a thermal evaporator. **d.** $1\ \mu\text{m}$ OFM apertures are punched on the Al thin film by the FIB machine.

In the current prototype device, instead of punching one line of apertures, we choose two rows of CMOS pixels spaced by another row, and punch two rows of corresponding apertures with $1\ \mu\text{m}$ diameter (Fig. 4a). The reason for this configuration is two fold. First, since the two OFM array are separated in the flow direction, they will take two sets of line profiles for the same specimen at a slightly different time. By knowing the distance between the two OFM arrays in the flow direction, the flow speed of the specimen can be calculated, which can be used to reconstruct two OFM images from the two sets of OFM line profiles correctly. Secondly, two OFM images of the same specimen are acquired by the two rows of OFM apertures. If the flow speed of the *C. elegans* is uniform, the reconstructed OFM images will be perfect and the cross correlation of the two OFM images is one. Uneven flow speed of the *C. elegans*, usually caused by the adhesion of the *C. elegans* to the channel wall, can introduce distortion in OFM images and reduce the cross correlation of the two OFM images. So the cross correlation of the two OFM images is used to verify the fidelity of the OFM images and to screen out distorted OFM images automatically.

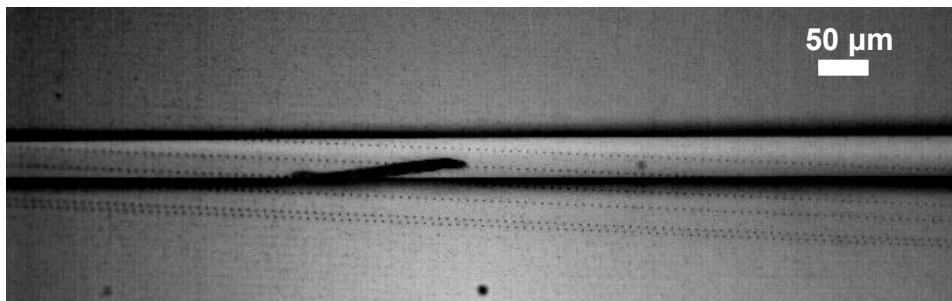
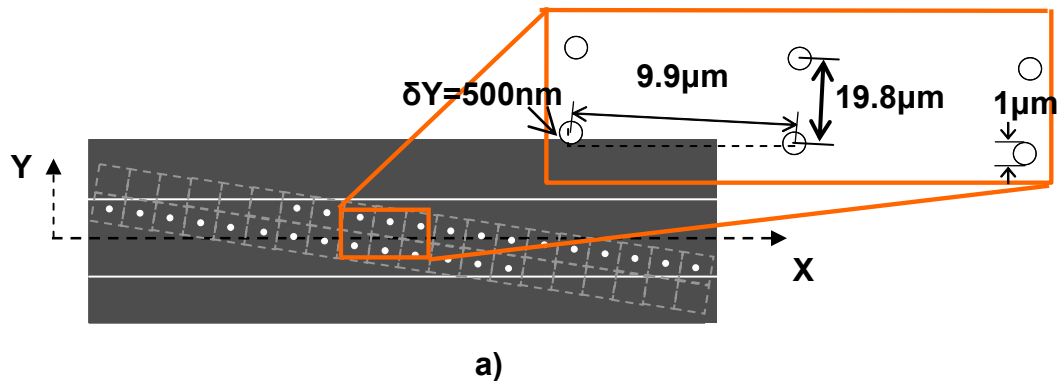
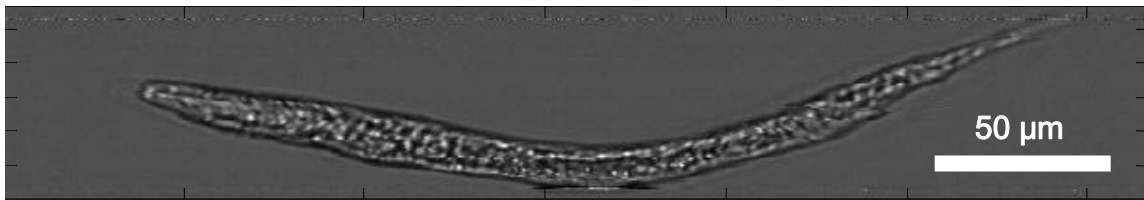


Figure 4: **a.** The configuration of two OFM arrays in the prototype device. **b.** A photo showing a *C. elegans* flowing across the two OFM arrays during the OFM imaging experiment.

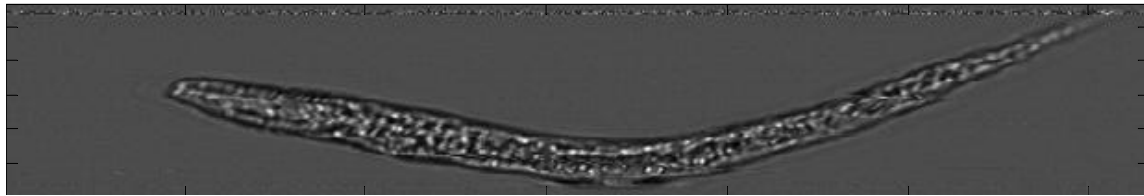
At the end, we bonded an optically transparent PDMS microfluidic chip on top of the Al coated CMOS sensor chip with a Suss mask aligner. The width of the microfluidic channel was 50 μm , and the height was 15 μm . The alignment set the apertures array oriented at a small angle θ with respect to the flow direction X , which ensured about 100 apertures in each row span across the microfluidic channel. We also spin-coated a 200 nm thick polymethylmethacrylate (PMMA) layer onto the Al film to protect the OFM apertures and improve the adhesion between the Al coated CMOS sensor and the PDMS microfluidic chip. Oxygen plasma was used to make the inner surface of the PDMS microfluidic channel hydrophilic. 10% polyethyleneglycol (PEG)⁶ was used in the experiment to reduce the adhesion of the *C. elegans* to the channel walls. The average flow speed of the sample was about 500 $\mu\text{m}/\text{sec}$. The illumination of the OFM was a collimated inherent white light ($\sim 20 \text{ mW cm}^{-2}$) emitted by a halogen lamp from above. The exposure time of the CMOS sensor was 0.9 ms, which yielded frame rate f about 1k Hz.

3. Experimental results

4.1 *C. elegans* imaging



a)



b)



Figure 5: a. Two OFM images of the same wild-type *C. elegans* L1 larva recorded by the two OFM arrays in the prototype device. **b.** A conventional microscope image of a *C. elegans* under a 20× objective.

Fig. 5a shows two OFM images of a wild-type *C. elegans* L1 larva taken by the two OFM arrays in our prototype device. The cross correlation between them is 60%. The specimen was immobilized in a 70 °C heat bath for 3 min. Consistent internal structures in both OFM images proves the consistency of the OFM imaging. For comparison to the conventional optical microscopy method, Fig. 5b shows a conventional microscope image of a wild-type *C. elegans* L1 larva taken by a 20× Olympus objective. The microscope image has a little better resolution than our OFM prototype device. But similar internal structures of *C. elegans* are shown in both microscope and OFM images, which confirms the fidelity of our OFM images.

4.2 Microsphere imaging

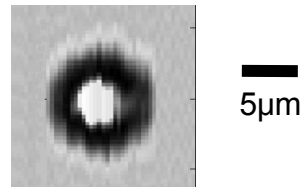


Figure 6: A OFM image of a 4.5 μm polystyrene microsphere.

Fig. 6 shows an OFM image of a 4.5 μm polystyrene microsphere (Polyscience Inc.). The microsphere is acting like a microlens. It focuses the light to a bright spot less than the size of the microsphere and induces a dark ring bigger than the size of the microsphere.

4. Conclusion and future work

In this paper, we have presented, as far as our knowledge, the world's smallest microscope device based on the OFM method. Both OFM images of *C. elegans* and microsphere confirm the OFM high resolution on-chip imaging capability.

Owe to the development of microfluidic technologies, it is possible to build a closed-loop microfluidic lab-on-a-chip system (Fig. 7.) that can incubate and perform automated imaging of a single nematode for life-cycle studies (e.g. days). Quantitative analysis of phenotypic variance is likely to be insightful in studying the effects of environment stress, nutrition and drugs on growth, reproduction, and life span of *C. elegans*.

Additional functionalities also can be built into the OFM systems. For example, the capability to perform fluorescence imaging can be added by simply depositing optical filters between the aperture array and the sensor array. In fact, the on-chip nature of the OFM easily enables multi-spectral analysis. A series of OFM device, each selective for a given wavelength band, can be built along a single microfluidic channel. Differential interference contrast (DIC) microscope also can be realized by punching two holes or four holes pairs to replace the single hole units in current device⁷.

The simplicity and compact nature of OFM systems, and the fact that they can be created with existing fabrication technology should translate to their swift adaptation as an important lab-on-a-chip component.

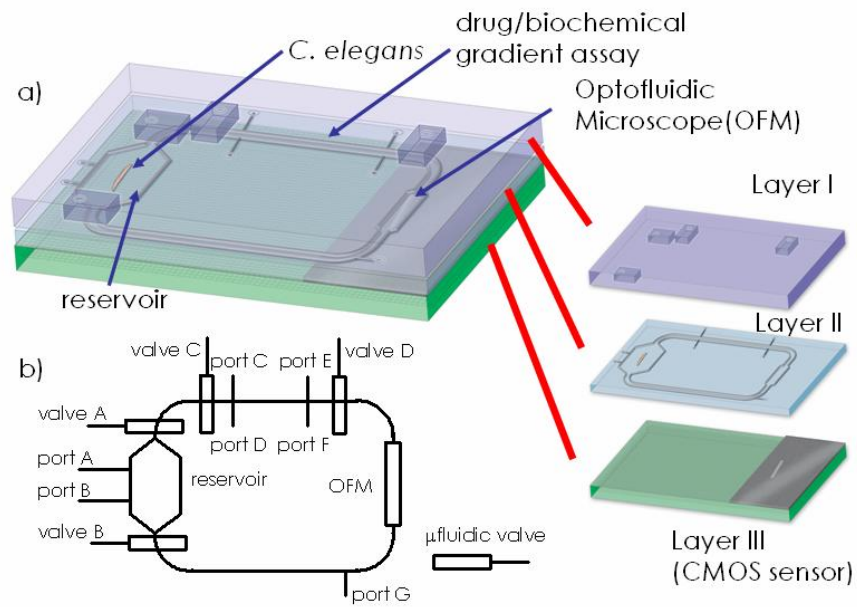


Figure 7: A closed-loop microfluidic lab-on-a-chip system that can incubate and perform automated imaging of a single nematode for life-cycle studies.

5. Acknowledgement

We are grateful for the generous help from Professor Axel Scherer. The assistance from Caltech Watson cleanroom is well appreciated. This project is funded by DARPA's center for optofluidic integration and Coulter Foundation Career Award.

REFERENCES

1. G. M. Whitesides, "The origins and the future of microfluidics," *Nature* **442**, 368-373 (2006).
2. J. El-Ali, P. K. Sorger, and K. F. Jensen, "Cells on chips," *Nature* **442**, 403-411 (2006).
3. X. Heng, D. Erickson, L. R. Baugh, Z. Yaqoob, P. W. Sternberg, D. Psaltis, and C. H. Yang, "Optofluidic microscopy - a method for implementing a high resolution optical microscope on a chip," *Lab on a Chip* **6**, 1274-1276 (2006).
4. D. Lange, C. W. Stormont, C. A. Conley, and G. T. A. Kovacs, "A microfluidic shadow imaging system for the study of the nematode *Caenorhabditis elegans* in space," *Sensors and Actuators B-Chemical* **107**, 904-914 (2005).
5. Y. Harada, T. Asakura, and T. Murakami, "SPATIAL AND TEMPORAL ANALYSIS OF SOLID-STATE IMAGING-SYSTEMS," *Applied Optics* **31**, 4758-4768 (1992).
6. S. W. Hu, X. Q. Ren, M. Bachman, C. E. Sims, G. P. Li, and N. Allbritton, "Surface modification of poly(dimethylsiloxane) microfluidic devices by ultraviolet polymer grafting," *Analytical Chemistry* **74**, 4117-4123 (2002).
7. M. Lew, X. Cui, X. Heng, and C. Yang, "Interference of a four-hole aperture for on-chip quantitative two-dimensional differential phase imaging," *Optics Letters* **32**, 3 (2007).